Organic Light-Emitting Diodes Based on 2-(Stilben-4-yl)benzoxazole Derivatives: An Implication on the Emission Mechanism

Chung-Wen Ko and Yu-Tai Tao*

Institute of Chemistry, Academia Sinica, Taipei, Taiwan 11529, Republic of China

Andrzej Danel, Lidia Krzemińska, and Piotr Tomasik

Department of Chemistry, University of Agriculture, Cracow, Poland

Received March 8, 2001. Revised Manuscript Received April 18, 2001

A series of 2-(stilben-4-yl)benzoxazole derivatives (BOXSB-X) was prepared and used as a dopant in the fabrication of organic light-emitting diodes. With a device structure of ITO/NPB/CBP/TPBI:3%BOXSB-X/TPBI/Mg:Ag, where NPB, CBP, and TPBI stand for 4,4′-bis[*N*-(1-naphthyl)-*N*-phenyl-amino]-biphenyl, 4,4′-dicarbazolyl-1,1′-biphenyl, and 2,2′,2″-(1,3,5-phenylene)tris-[1-phenyl-1H-benzimidazole], respectively, light emission from the dopant was observed under electric bias, presumably due to energy transfer between the host TPBI exciton and the dopant. Bright blue emission with a luminance ranging between 8 000 and 13 000 cd/m^2 was obtained depending on the substituent on the stilbene moiety. However, with a device structure of ITO/NPB/TPBI:3%BOXSB-X/TPBI/Mg:Ag, where no CBP layer was present, the recombination/emission region shifted to the NPB layer except in the device doped with dimethylamino-substituted benzoxazole derivative, in which case the carrier trap mechanism is suggested to be responsible for the emission from the dopant.

Introduction

Organic light-emitting diodes (OLEDs) have been investigated extensively in recent years for their potential applications in full-color flat-panel displays.[1] Improving the performance of OLEDs is an ongoing task in approaching the commercialization of this technology. Since Tang et al. reported that use of laser dye dopant in tris(8-hydoxyquinoline) aluminum (Alq) could enhance the efficiency and stability of OLEDs,[2] doping luminescent dyes into a charge carrier layer became a popular and effective way for achieving better performance and tuning the color.[3] Many highly fluorescent materials were developed to fulfill the need of three basic colors, red, green, and blue, for a full-color display. Among these, an efficient blue emission is one of the most sought-after colors. Although a number of blue OLEDs with high brightness have been reported recently,[4] new blue materials still attract much attention.

Heterocycles containing oxazole, oxadiazole, benzazole, and benzoxazole moieties were often found in the molecular structures of many fluorescent whitening agents or laser dyes.[5,6] Their luminescent properties (quantum yield, emission wavelength,) are much affected by substitution and/or extension of conjugation at the 2-position of the oxazole ring.[6] For example, 2-phenylbenzazole fluoresces in the UV region. Introduction of various substituents at the *p*-position of the phenyl ring causes enhancement of quantum yield and bathochromic shifts. Several benzoxazoles have been studied as emitters in electroluminescent (EL) devices.[7]

In this paper, we examined the physical properties of a series of blue fluorescent 2-(stilben-4′-yl)benzoxazole derivatives with various substituents on the stilbene moiety (BOXSB-X **1**−**4**, structures are shown in Figure 1) and evaluate the EL behavior in a multilayer device with these derivatives as the dopant in the electron-transporting layer (ETL) of TPBI. Highly bright blue or blue-green devices were obtained, depending on the dopant. By examination of the electroluminescence in different device configurations, a suggestion was made about the emission mechanism. Thus, under a device structure of ITO/NPB/CBP/TPBI:3%BOXSB-X/TPBI/

* To whom correspondence should be addressed.

(1) (a) Kido, J. *Bull. Electrochem.* **1994**, *10*, 1. (b) Sheats, J. R.; Antoniadis, H.; Hueschen, M.; Leonard, W.; Miller, J.; Moon, R.; Roitman, D.; Stocking, A. *Science* **1996**, *273*, 884. (c) Rothberg, L. J.; Lovinger, A. J. *J. Mater. Res.* **1996**, *11*, 3174. (d) Dodapalapur, A. *Solid State Commun.* **1997**, *102*, 259. (e) Mitschke, U.; Bäuerle, P. *J. Mater. Chem.* **2000**, *10*, 1471.

(2) Tang, C. W.; Van Slyke, S. A.; Chen, C. H. *J. Appl. Phys.* **1989**, *65*, 3610.

(3) (a) Adachi, C.; Tsutsui, T.; Saito, S. *Appl. Phys. Lett.* **1990**, *56*, 799. (b) Adachi, C.; Tokito, S.; Tsutsui, T.; Saito, S. *Jpn. J. Appl. Phys.* **1988**, *28*, L269. (c) Shoustikov, A. A.; You, Y.; Thompson, M. E. IEEE *J. Sel. Top. Quantum* **1998**, *4*, 3. (d) Tao, Y. T.; Balasubramaniam, E.; Danel, A.; Jarosz, B.; Tomasik, P. *Appl. Phys. Lett.* **2000**, *77*, 1575.

(4) (a) Hosokawa, C.; Higashi, H.; Nakamura, H.; Kusumoto, T. *Appl. Phys. Lett.* **1995**, *67*, 3853. (b) Gao, Z.; Lee, C. S.; Lee, S. T.; Chen, R. M.; Luh, T. Y.; Shi, J.; Tang, C. W. *Appl. Phys. Lett.* **1999**, *74*, 865. (c) Tao, Y. T.; Balasubramaniam, E.; Danel, A.; Tomasik, P. *Appl. Phys. Lett.* **2000**, *77*, 933.

(5) (a) Siegrist, A. E.; *Helv. Chim. Acta* **1967**, *50*, 906. (b) Siegrist, A. E.; Hefti, H.; Meyer, H. R.; Schmidt, E. *Rev. Prog. Coloration* **1987**, *17*, 39. (c) Fletcher, I. J.; Siegrist, A. E. *Adv. Heterocycl. Chem.* **1978**, *23*, 171.

(6) Krasovitskii, B. M.; Bolotin, B. M. *Organic Luminescent Materials*; VCH: Weinheim, 1988.

(7) (a) Saitoh, Y.; Matsuoka, M.; Nakao, Y.; Kitao, T. *Chem. Lett.* **1991**, 285. (b) Chen, C. H.; Shi, J.; Tang, C. W. *Macromol. Symp.* **1997**, *125*, 1.

10.1021/cm010199u CCC: $20.00
Published on Web 06/07/2001

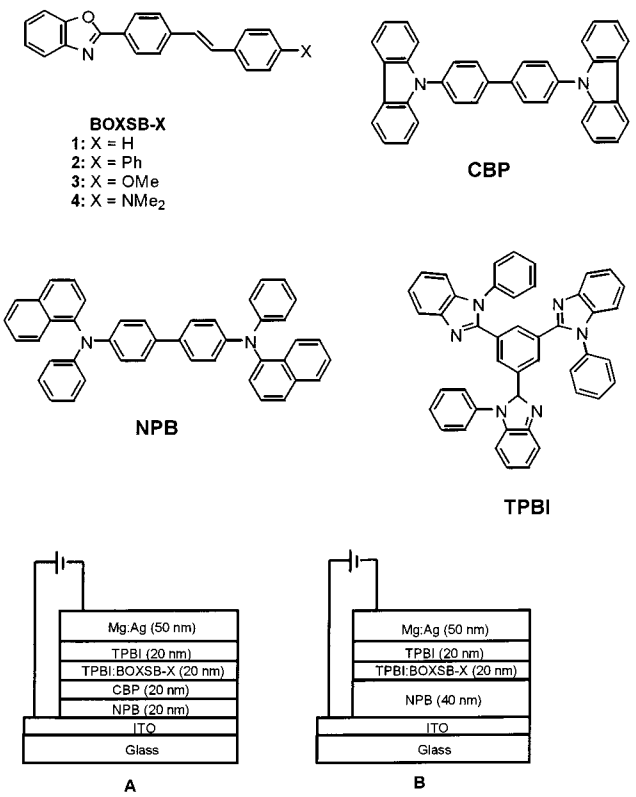

Figure 1. Device structure and materials used in this study.

Mg:Ag, where NPB, CBP, and TPBI stand for 4,4′-bis-[*N*-(1-naphthyl)-*N*-phenylamino]biphenyl, 4,4′-dicarbazolyl-1,1′-biphenyl, and 2,2′,2″-(1,3,5-benzenetriyl)-tris-[1-phenyl-1H-benimidazole], respectively, the dopants were excited and emitted fluorescent light through Förster energy transfer from the host TPBI exciton. On the other hand, under a device structure of ITO/NPB/TPBI:3%BOXSB-X/TPBI/Mg:Ag, where no CBP is inserted, the origin of light emission depends on the dopant. With **1**, **2**, or **3** as the dopant, a blue EL emission came from the hole-transporting layer (HTL) of NPB due to the hole-blocking effect of TPBI. With **4** as the dopant, EL emission from **4** was observed, presumably because of carrier trapping by the dopant molecules.

Experimental Section

Materials. The variously substituted 2-(stilben-4-yl)benzoxazole derivatives **1**−**4** were prepared by following the Anil synthesis reported by Siegrist.[5a] Thus, the 2-(*p*-tolyl)-benzoxazole (0.01 mol) and the Schiff base of appropriate aromatic benzaldehyde were dissolved in anhydrous DMF and potassium *tert*-butoxide (0.015 mol) was added. The reaction mixture was stirred at 50 °C for 3 h. After cooling, it was poured into water and acidified with 10% HCl. The precipitate was filtered off, dried, and recrystallized from DMF. Products were characterized by NMR and compared with literature data.

*E-2-(Stilben-4-yl)-benzoxazole (**1**).* Colorless plates, 58%, mp 197−199 °C, lit.[5] 199−199.5 °C.[1]H NMR (300 MHz, $CDCl_3$): δ 7.14 (d, J = 16.2 Hz, 1H), 7.23 (d, J = 16.5 Hz, 1H), 7.30 (t, J = 7.4 Hz, 1H), 7.34−7.41 (m, 4H), 7.55 (d, J = 7.1 Hz, 2H), 7.57−7.59 (m, 1H), 7.65 (d, J = 8.2 Hz, 2H), 7.76−7.79 (m, 1H), 8.23 (d, J = 8.5 Hz, 2H).

*E-2-(4-Phenylstilben-4′-yl)-benzoxazole (**2**).* Greenish plates, 46%, mp 275−276 °C, lit.[5] 276−276.5 °C. [1]H NMR (300 MHz, DMSO): δ 7.34−7.43 (m, 7H), 7.68−7.80 (m, 8H), 7.83 (d, J = 8.2 Hz, 2H), 8.19 (d, J = 8.2 Hz, 2H).

*E-2-(4-Methoxystilben-4′-yl)-benzoxazole (**3**).* Pale yellow needles, 51%, mp 217−220 °C, lit.[5] 220.5−222 °C. [1]H NMR (300 MHz, $CDCl_3$,): δ 3.84 (s, 3H, OCH_3), 6.92 (d, J = 8.5 Hz, 2H), 7.02 (d, J = 16.2 Hz, 1H), 7.02 (d, J = 16.2 Hz, 1H), 7.33−7.36 (m, 2H), 7.49 (d, J = 8.8 Hz, 2H), 7.55−7.60 (m, 1H), 7.63 (d, J = 8.5 Hz, 2H), 7.74−7.80 (m, 1H), 8.23 (d, J = 8.5 Hz, 2H).

*E-2-(4-N,N-Dimethyl-stilben-4′-yl)-benzoxazole (**4**).* Yellow crystals, 35%, mp 274−276 °C. [1]H NMR (300 MHz, DMSO): δ 2.95 (s, $-N(CH_3)_2$, 6H), 6.74 (d, J = 8.8 Hz, 2H), 7.03 (d, J = 16.2 Hz, 1H), 7.29 (d, J = 16.2 Hz, 1H), 7.36−7.43 (m, 2H), 7.46 (d, J = 8,8 Hz, 2H), 7.69−7.78 (m, 4H), 8.13 (d, J = 8.5 Hz, 2H). Anal. Calcd for $C_{23}H_{20}N_2O$: C, 81.15; H, 5.92; N, 8.23. Found: C, 81.36; H, 5.77; N, 8.12.

The charge-transporting materials α-NPB, CBP, and TPBI were all prepared according to literature procedures[8] and subjected to gradient sublimation prior to use.

Instrumentation. Absorption and emission spectra were taken with Hewlett-Packard 8453 absorption spectrophotometer and Hitachi F-4500 fluorescence spectrophotometers, respectively. Cyclic voltammetric experiments were carried out using a BAS 100B electrochemical analyzer. A conventional three-electrode cell system was used, with glassy carbon, a platinum wire, and Ag/AgCl as the working, counter, and reference electrode, respectively. Degassed dichloromethane solution with 0.1 M tetra-*n*-butylammonium haxafluorophosphate was used as the electrolyte medium.

Device Fabrication and Characterization. The substrate was an indium tin oxide (ITO) coated glass, with a sheet resistance of <50 Ω/sq[2], was obtained from Merck Display Technology, Taiwan. The ITO substrates were prepatterned with an effective emitting area of 3.14 mm[2]. The pretreatment of ITO included routine sonication in a detergent solution and then water and alcohol in sequence. Oxygen plasma cleaning (1 min) was performed before loading the substrates into the deposition chamber. The thermal evaporation of organic materials was carried out using ULVAC Cryogenics at a chamber pressure of 2×10^{-6} Torr. The thickness of each layer is indicated in Figure 1. For the doped TPBI:BOXSB-X layer, the dye concentration was kept around 3 wt % or as indicated in the text by coevaporating from a different thermal source with TPBI. The second layer of TPBI was used here to protect the luminescent layer from cathode deposition, where the penetration of a hot metallic layer is expected in organic material for a few nanometers.[9] The cathode Mg:Ag (10:1, 50 nm) alloy was deposited by coevaporation. A thick layer (≈100 nm) of silver capping layer was finally deposited. The current, voltage, and light intensity ($I-V-L$) measurements were made simultaneously using a Keithley 2400 Source meter and a Newport 1835C Optical meter equipped with a Newport 818-ST silicon photodiode. The measurements were made at room temperature and ambient conditions. The electroluminescence (EL) spectra were taken using the fluorescence spectrophotometer with the incident light blocked from entering the sample compartment. For the necessary cases, a parallel deposition was carried out at the same time on a glass slide to measure the photoluminescence (PL) spectra of solid films.

Results and Discussion

Optical Properties. The UV−vis absorption spectra of the four dyes in CH_2Cl_2 solution are shown in Figure 2. The λ_{max} data are listed in Table 1. The absorption peak occurs between 300 and 400 nm except for **4**, which has the absorption spans from 250 to 450 nm, with two major absorptions. A substituent effect can be seen from the data. Red shifts were observed in going from **1** to **2** and **3** and **4**. Thus, the donating group shifts the

(8) (a) Koene, B. E.; Loy, D. E.; Thompson, M. E. *Chem. Mater.* **1998**, *10*, 2235. (b) Shi, J.; Tang, C. W.; Chen, C. H. U.S. Patent 5,645,948, 1997. (c) Chen, C. H.; Shi, J. *Coord. Chem. Rev.* **1998**, *171*, 161.

(9) Lee, S. T.; Gao, Z. Q.; Hung, L. S. *Appl. Phys. Lett.* **1999**, *75*, 1404.

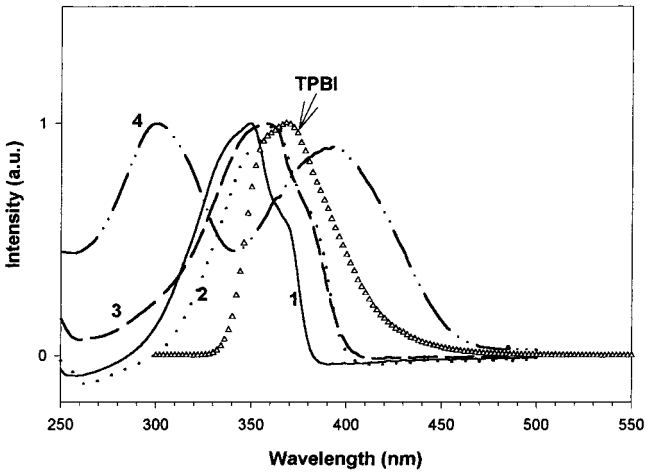

Figure 2. UV−vis absorption spectra of BOXSB-X **1**−**4**; also included is the emission spectrum of TPBI.

Table 1. Photophysical Properties of the BOXSB-X Derivatives

BOXSB-X	λ_{max} abs in CH_2Cl_2 (nm)	λ_{max} EM in CH_2Cl_2 (nm)	λ_{max} EM (solid film) (nm)	HOMO (eV)	LUMO (eV)	quantum yield[a] (%)
1	349	402	448	6.0	2.8	0.99
2	362	426	446	5.9	2.8	0.94
3	358	430	462	5.7	2.7	0.23
4	393	518	540	5.1	2.5	0.13

[a] The quantum yield of BOXSB-X was measured in CH_2Cl_2 by using 9,10-diphenylanthracene as a reference (QY = 1).

absorption to a longer wavelength, with the dimethylamino group causing the biggest shift. This substitution effect is in agreement with molecular orbital calculation (AM1), which shows that, in the LUMO, the electron density is localized more in the phenyl ring directly connected to the 2-position of the benzoxazole unit. Whereas in the HOMO, substantial electron density is found in the terminal phenyl ring in the stilbene moiety. A donating group at the 4-position of this ring is expected to raise the energy of the HOMO more than that of the LUMO so that the energy gap is lowered. A similar trend is observed in the photoluminescence in CH_2Cl_2. As shown in Figure 3, the peak of emission shifts to a longer wavelength with stronger donating groups. For the parent compound **1**, the emission has a peak maximum at 402 nm, with several apparent vibronic features, whereas for dimethylamino-substituted **4**, the emission maximum moves to the green region at 518 nm. Photoluminescence in cyclohexane and ethyl acetate was also examined. Little solvatochromism is observed for compound **1**, whereas compound **4** exhibits the strongest solvatochromism. The emission maximum of **4** in cyclohexane occurs at 402 nm, with clear vibronic features. Again, this is in accord with the MO calculation. The ground-state molecular dipole moment increases in the order of **1** < **2** < **3** < **4**, with the dipole pointing more or less along the molecular axis toward the benzoxazole ring. Upon UV excitation, a more polar excited state is expected. Thus, a polar solvent stabilizes the excited state more than the ground state. This effect is most significant with compound **4**. The PL of the solid films reflects a similar substituent effect on emission λ_{max} (Table 1). Furthermore, all four compounds give a solid film PL that is 20−30 nm red-

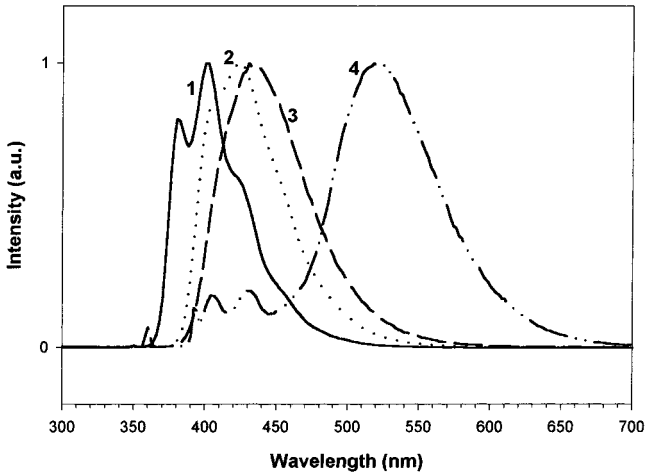

Figure 3. Photoluminescence spectra of BOXSB-X **1**−**4**.

shifted relative to respective PL in CH_2Cl_2. Molecular modeling also showed that these compounds are rather flat, so that packing and thus the bathochromic shift or excimer formation in the solid state is not surprising. The quantum yields of these dyes in CH_2Cl_2 were estimated with diphenylanthracene as a standard ($\varphi_f = 1$).[10] It is noted that the highest quantum yield was observed for compound **1** and decreases with the introduction of electron-donating groups. This appears to correlate with the solvatochromism found for the series: a larger red shift was found for molecules with stronger electron-donating groups. It is suggested that a stronger intermolecular interaction with the solvent quenches the excited state more readily.

Electrochemical Properties. The redox behaviors of the four dyes were determined by cyclic voltammetry in dichloromethane. All four show irreversible redox behavior: an oxidation peak appeared during an oxidative scan but only a small peak was found in the reverse scan. This suggests that these compounds have an unstable oxidized form under electrochemical conditions. The oxidation potential decreases in the order of **1** > **2** > **3** > **4**. This is the order expected from the nature of the substituents: the ones with donating groups are oxidized more readily. The HOMO levels are calculated from the oxidation potential by adding 4.4.[11] Using the UV absorption edge to estimate the energy gap, the LUMO levels are also calculated and listed in Table 1.

Electroluminescent Behavior. To serve as a dopant, it is generally believed that a spectral overlap between the host emission and the dopant absorption is desirable to ensure an efficient Förster energy transfer.[12] With these blue to blue-green emitters, a wide band-gap electron-transfer material, TPBI, was chosen as the host. As shown in Figure 2, the spectral overlap of the PL emission of TPBI and the absorption spectra of BOXSB-X was reasonable. The HOMO and LUMO energy levels of BOXSB-X are also located within the HOMO and LUMO energy levels of TPBI, except for **4**,

(10) Morris, J. V.; Mahaney, M. A.; Huber, J. R. *J. Phys. Chem.* **1976**, *80*, 969.
(11) Janietz, S.; Bradley, D. D. C.; Grell, M.; Giebeler, C.; Inbasekaran, M.; Woo, E. P. *Appl. Phys. Lett.* **1998**, *73*, 2453.
(12) (a) Förster, T. *Discuss Faraday Soc.* **1959**, *27*, 2. (b) Kido, J.; Shionoya, H.; Nagai, K. *Appl. Phys. Lett.* **1995**, *67*, 2281.

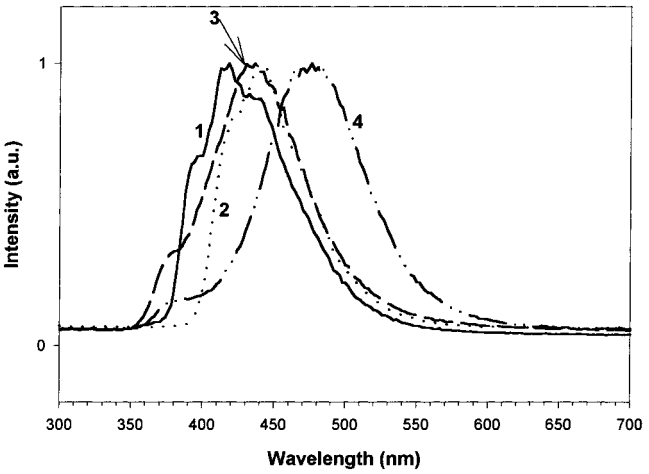

Figure 4. EL spectra of devices ITO/NPB/CBP/TPBI: 3%BOXSB-X/TPBI/Mg:Ag/Ag.

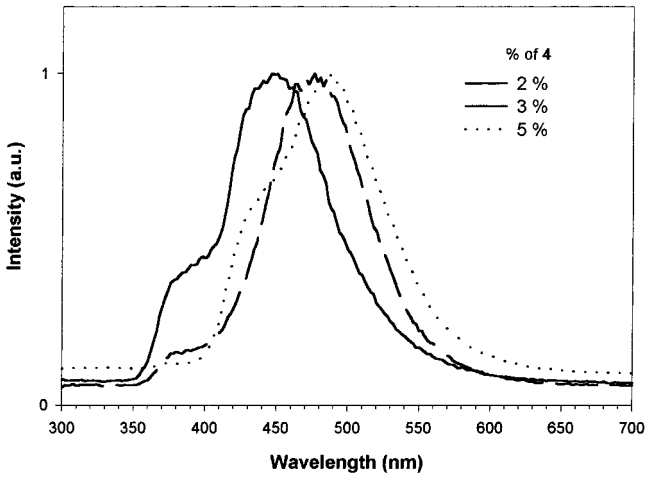

Figure 5. EL spectra as a function of dopant concentration in a device of ITO/NPB/CBP/TPBI:**4**/TPBI/Mg:Ag/Ag.

whose LUMO (at 2.5 eV) is slightly higher than the LUMO of TPBI (at 2.7 eV).

Our previous works have shown that, with a device structure of ITO/NPB/TPBI/Mg:Ag, the exciton formation occurs in the NPB layer ($\lambda_{max} = 445$ nm) due to a large band gap between the HOMOs of NPB and TPBI so that the TPBI serves as a hole blocker.[4c] When a second hole-transporting layer CPB was inserted between the NPB layer and the TPBI layer, the recombination region shifts mainly to the TPBI layer to give an EL that is dominated by the emission of TPBI at 376 nm, together with minor emission from NPB/CBP. The CBP layer provides an intermediate level for holes to transport through to the TPBI layer. In the current work, we tried two device configurations. When a multilayer device with the configuration of ITO/NPB(20 nm)/CBP(20 nm)/TPBI:3%BOXSB-X(20 nm)/TPBI(20 nm)/Mg:Ag(50 nm)/Ag(100 nm) were fabricated, the EL spectra (Figure 4) gave a similar substituent dependence as the PL spectra for the identically doped films in both peak position and shape, confirming the origin of emission to be the dopant. The emission λ_{max} of devices based on **1**−**4** was at 418, 440, 436, and 476 nm, respectively. It is noted, however, the EL emission of the **4**-doped device was blue-shifted about 14 nm with respect to the corresponding PL emission. A spectrum simulation showed that this shift might be due to a partial contribution of emission from NPB at ≈445 nm. A small shoulder at around 375 nm, which also occurs in the corresponding PL spectrum, is attributed to the host emission of TPBI due to an incomplete energy transfer. Thus, energy transfer from the host TPBI to the dopant is mainly responsible for the emission. Raising the concentration of the dopant to 5% resulted in complete elimination of this shoulder (Figure 5). A bathochromic shift in the emission λ_{max} was also seen with increasing dopant concentration. This can be attributed to the increasing dielectric constant of the medium as a result of an increasing amount of more polar dopant of **4**.[13]

The current−voltage−luminance ($I-V-L$) characteristics measured at room temperature under ambient conditions were shown in Figure 6. Very bright emission

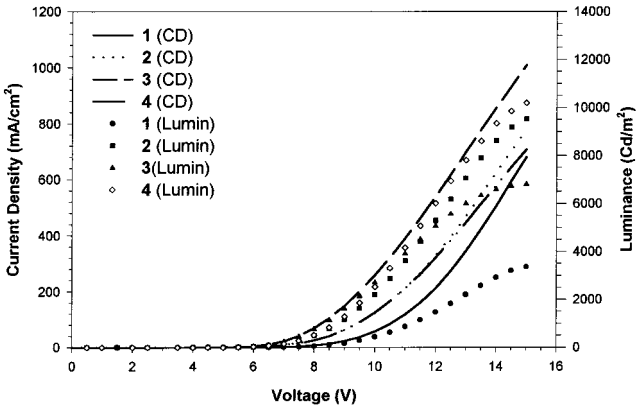

Figure 6. $I-V-L$ curves for the devices ITO/NPB/CBP/TPBI: 3%BOXSB-X/TPBI/Mg:Ag/Ag.

was obtained for these dyes. For instance, the maximum brightness ranges between 3 370 cd/m^2 for the **1**-doped device to 10 200 cd/m^2 for the **4**-doped device. Raising the concentration of dopant **4** to 5% further raises the maximum luminance to 13 000 cd/m^2 (at 15 V). The device doped with 3% of **2** gave a maximum luminance of 9 500 cd/m^2 at 15 V and a maximum quantum efficiency of 2.1% at 42 mA/cm^2. The power efficiency ranges between 0.3 and 1.0 lm/W, with no clear correlation with the electronic properties of the substituent. At a current density of 100 mA/cm^2, the luminance reaches 740, 1800, 1080, and 2083 cd/m^2 for **1**, **2**, **3**, and **4**, respectively. At 20 mA/cm^2, the luminance dropped proportionally to ≈20% of the values at 100 mA/cm^2. It should be noted that the brightness depends on the peak position, in addition to other factors such as fluorescence quantum yield. Thus, while compound **1** has the highest PL quantum efficiency, the lowest brightness for the **1**-based device may be due to its purple emission peak, which is farther away from the photopic vision curve of human eyes. A summary of the performance of various devices is shown in Table 2.

In another device configuration ITO/NPB/TPBI: 3%BOXSB-X/TPBI/Mg:Ag, where the CBP layer is eliminated, the EL spectra are somewhat different from above (Figure 7). It is interesting to note that devices doped with **1**−**3** gave overlapping EL spectra. This EL spectrum also coincides with that of an ITO/NPB/TPBI/Mg:Ag device, which was shown to give EL from a NPB

(13) Bulovic, V, Deshpande, R.; Thompson, M. E.; Forrest, S. R. *Chem. Phys. Lett.* **1999**, 308, 317−322.

Table 2. Device Performance of ITO/NPB/CBP/TPBI:BOXSB-X/TPBI/MgAg

	@100 mA/cm^2					
BOXSB-X	voltage (V)	luminance (cd/m^2)	max. luminance (cd/m^2)	max. quantum efficiency (%)	max. power efficiency (lm/W)	CIE (x,y)
3% **1**	10.7	740	3370@15.0V	1.10@8.5V	0.30@7.5V	0.18, 0.11
3% **2**	9.6	1800	9530@15.0V	2.07@8.5V	0.78@7.0V	0.18, 0.12
3% **3**	8.4	1080	6810@15.0V	1.25@8.5V	0.46@6.5V	0.18, 0.12
3% **4**	9.6	2030	10200@15.0V	1.36@9.5V	0.77@8.0V	0.18, 0.23
5% **4**	8.7	1810	13300@15.0V	1.26@6.5V	1.02@6.0V	0.20, 0.28

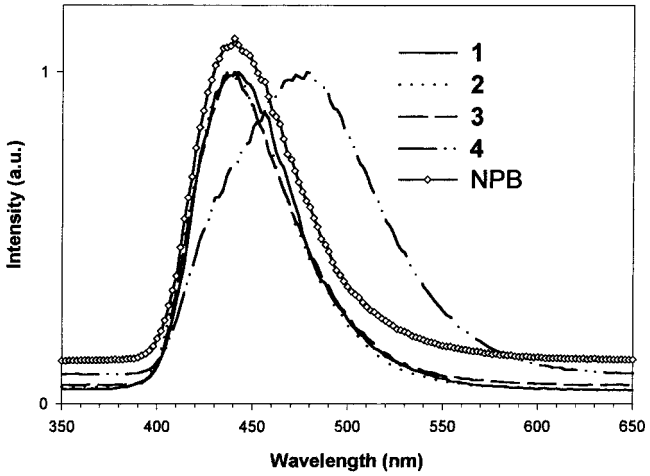

Figure 7. EL spectra of device ITO/NPB/TPBI:3%BOXSB-X/TPBI/Mg:Ag/Ag. Also included is the EL spectrum for the same device without a dopant.

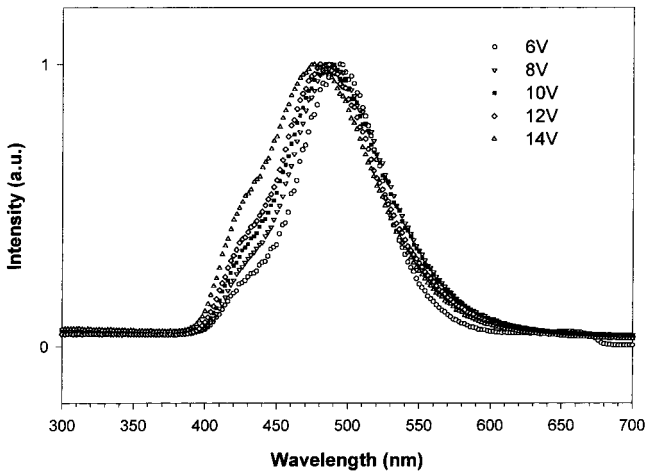

Figure 8. EL spectra of device ITO/NPB/CBP/TPBI:**4**/TPBI/Mg:Ag/Ag as a function of applied voltages.

layer.[4c] Thus, for devices with these dopants, the recombination region, and thus exciton formation, are still within the NPB layer, presumably due to the large gap between HOMOs of NPB and TPBI. Only compound **4** gave an EL spectrum that is identified as coming from the dopant. It is also noted that in the EL there is no emission contribution from the host TPBI. This is in contrast to the small shoulder from TPBI in the EL in cases where a CBP layer was inserted. The shape of this EL spectrum appears to encompass a shoulder due to the emission of NPB. When the applied voltage increases, the contribution from NPB emission also increases (Figure 8). It is suggested that the emission is not due to the host−guest energy transfer. Instead, it is due to charges trapped in the dopants. While the holes cannot cross to the HOMO of the TPBI host, they can cross directly into the HOMO of the dopant and be

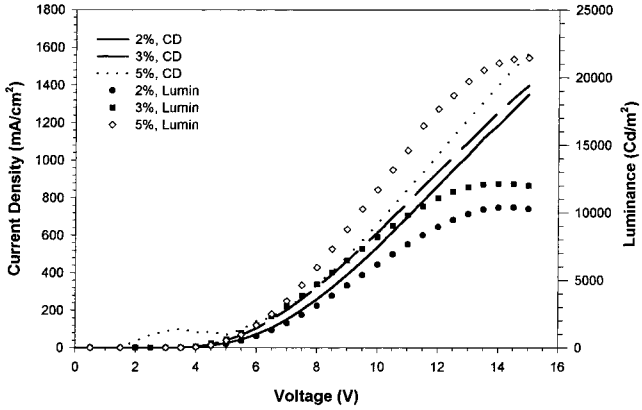

Figure 9. $I-V-L$ characteristics of device ITO/NPB/TPBI:**4**/TPBI/Mg:Ag/Ag with different dopant concentrations.

trapped there. Then, electrons in the LUMO of dopants combined with these holes to form excitons. As the voltage increases, more electrons are injected from the LUMO of TPBI to that of NPB, as the traps are limited by the low concentration and may get saturated at higher electron flux. It is noted that both the current density and the luminance for the device without a CBP layer is higher than that with a CBP layer at the same dopant concentration and are increasing with increasing dopant concentration (from 2% to 5%). With 5% dopant of **4**, the device without a CBP layer reached a current density of ≈1 500 mA/cm^2 and a maximum luminance more than ≈20 000 cd/m^2(Figure 9).

Then, the question arises as to why, in cases of dopants **1**−**3**, the holes were stopped at the NPB/TPBI interface, but in the case of **4**, the holes can cross the interfacial barrier and excitons of the dopant can be formed. An examination of the energy alignment of various layers may reveal some clues. The situations for **1**−**3** are represented by compound **2** in Figure 10a. The barrier for holes to cross to the HOMO of either TPBI or the dopant is large compared to the barrier for electrons crossing from the LUMO of TPBI to that of NPB. Thus, electron/hole recombination occurred in NPB. Whereas in Figure 10b, a smaller energy gap between the HOMO of NPB and that of dopant **4** allowed holes to cross over directly from NPB to the dopants. This picture is also in agreement with our earlier report using other blue dopants in TPBI,[4c] where in two-layer devices with several blue dopants in TPBI, only the emission from NPB was observed. The presence of a CBP layer changed the various interfacial barriers so that the formation of excitons of TPBI followed by energy transfer to various dopants are dominating, with some electron leaking to the NPB layer as well. At higher voltage, this leakage increases and the emission from NPB also increases. This situation is illustrated in Figure 10c.

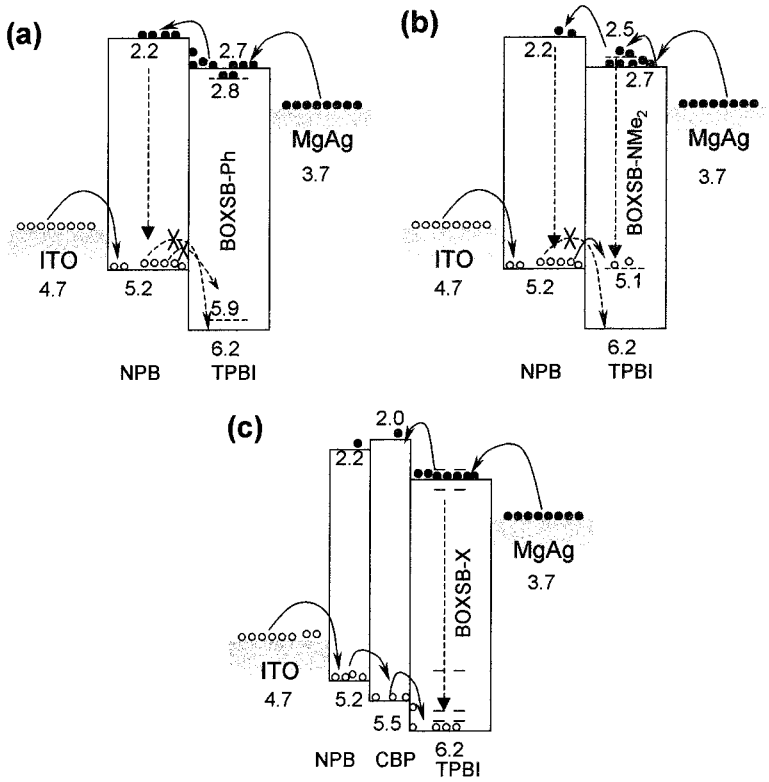

Figure 10. HOMO/LUMO energy alignment of various layers and suggested charge-transporting processes in (a) the device involving compound **2**, (b) the device involving compound **4** in the absence of a CBP layer, and (c) the device involving all dopants in the presence of a CBP layer.

Conclusion

In conclusion, we have demonstrated the bright-blue organic light-emitting devices from a series of benzoxazole derivatives BOXSB-X when used as the emissive dopant in a multilayer OLED fabrication. The emission mechanism may vary, depending on the device configuration. With a device structure of ITO/NPB(20 nm)/CBP(20 nm)/TPBI:3%BOXSB-X(20 nm)/TPBI(20 nm)/Mg:Ag(50 nm)/Ag(100 nm), the energy transfers from TPBI host excitons to the dopants and thus emission from the dopants is obtained. Under this configuration, a maximum brightness of more than 10 000 cd/m^2, a maximum external quantum efficiency of more than 2%, and a maximum power efficiency of 0.8 lm/W could be achieved for these blue fluorescent devices. In the device structure of ITO/NPB(40 nm)/TPBI:3%BOXSB-X(20 nm)/TPBI(20 nm)/Mg:Ag(50 nm)/Ag(100 nm), the EL depends on the dopant involved. For benzoxazoles **1**−**3**, the emission came from the hole-transporting NPB layer. Emission from dopant **4** was found, nevertheless, due to a carrier trap mechanism. Higher current and luminance were obtained compared to those of a similar device with a CBP layer inserted between the NPB and TPBI layers. Thus, the introduction of an additional hetero-junction with CBP may provide an advantage in terms of barrier crossing but not necessarily in the current flow. Whether this is due to a lower hole mobility for the CBP or the extra interface in hole transporting is being explored in our laboratory.

Acknowledgment. Financial support from a Theme Research Grant of the Academia Sinica of the Republic of China and a grant from the Polish Scientific Committee (Grant 8 T11B 075 18) are gratefully acknowledged.

CM010199U